

Energy Requirements for a Chemical Reaction. 2. Electron Transfer to SbF_5 and SnCl_4

J. F. Hershberger,[†] Y. D. Huh, J. J. McAndrew,[‡] R. J. Cross,* and M. Saunders*

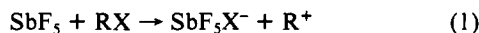
Contribution from the Department of Chemistry, Yale University, Box 6666, New Haven, Connecticut 06511. Received July 27, 1987

Abstract: We have measured the integral reactive cross section for the electron-transfer reaction $A + D \rightarrow A^- + D^+$, where the electron acceptor A is SnCl_4 or SbF_5 and the electron donor D is one of three amines. By using seeded nozzle beams we are able to vary separately the translational and vibrational energies. The cross sections rise rapidly above a threshold which is equal to or just above the thermodynamic, adiabatic threshold for the reaction. Vibrational energy in this region plays little or no role in the reaction. At higher energies the dependence on translational energy levels off and then drops rapidly. In this region an increase in vibrational energy makes a large increase in the cross section. At high energies, some of the product ions dissociate. The ratios of the intensities of the various products depends largely on translational energy even though the overall cross section depends markedly on vibrational energy.

Energy flow during a chemical reaction is one of the important features in chemical dynamics. Energy does not appear randomly in the different modes of the products, and different types of energy in the reactants may affect the course of the reaction in very different ways. For example, the earliest beam experiments on the reactions of alkali atoms with halogens showed that energy was released primarily as vibration in the alkali halide product.¹ Using a chemical laser Brooks showed that the reactive cross section of potassium with vibrationally excited HCl was much higher than the cross section for unexcited HCl with a comparable amount of translational energy.^{2a} Heismann and Loesch^{2b} found similar results at low energy for $\text{K} + \text{HCl}$ and for $\text{K} + \text{HF}$. Chupka et al. were able to measure the reactive cross sections of H_2^+ in various vibrational quantum states as functions of translational energy.³ Zare et al. were able to measure the vibrational quantum state of the BaF product in the reaction of $\text{Ba} + \text{HF}$ as a function of the vibrational state of HF .⁴

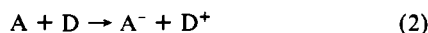
We have used crossed seeded nozzle beams to vary the amount and type of the energy of the reactants. The beams are prepared with a low Mach number (7-10) so that vibrational cooling is minimized. To a rough approximation, the vibrational energy distribution in the beam is given by a Boltzmann distribution at the nozzle temperature, which can be varied. The translational energy can be varied by changing the nozzle temperature, the type of carrier gas, or the beam intersection angle.

We have previously reported results by using this technique on two systems. In the dioxetane reaction, the reaction of excited O_2 ($^1\Delta_g$) with olefins, the reactive cross section increases rapidly as the relative translational energy is increased above the threshold, but vibrational excitation in the olefin has little effect.⁵ In the halide abstraction reactions of SbF_5 ,^{6,7}



at energies above the threshold, the cross section again rises rapidly with translational energy above the threshold. Vibrational energy in RX does not play a major role over most of the energy range studied. Close to the threshold, however, it may be very important. We have found two cases where the R^+ product can dissociate, and, in these cases, vibrational energy in the RX reactant is very important in this dissociation.

In this paper we look at the effects of different amounts and kinds of energy on the electron-transfer reactions



where the electron acceptor A is a metal halide, SbF_5 , or SnCl_4 , and the donor D is an amine. Electron transfer between an ion

and a neutral, charge exchange is, of course, very common.⁸ Electron transfer between two neutrals has been known for some time but is not as well studied^{9,10} in the gas phase. We have previously studied the dynamics of reaction 2, looking at the angular and energy distributions of the products.¹¹ Except at low energies, the reaction goes by way of a modified stripping process. The two reactants pass each other in a grazing collision, and an electron jumps from D to A. The ion products then separate and are slowed by their mutual Coulomb attraction. We can define both a vertical and an adiabatic ionization potential of D, IP_{vert} and IP_{ad} , where IP_{ad} is the difference in energies between the ground state of D^+ and the ground state of D and where IP_{vert} is the difference in energy between the ground state of D and the point on the potential surface of the D^+ directly above the ground state of D. They will differ unless all the bond lengths and angles in D^+ are the same as those in D. Similarly, we can define a vertical and an adiabatic electron affinity of A, EA_{vert} and EA_{ad} . The absolute threshold energy for the reaction is $E_{\text{ad}} = \text{IP}_{\text{ad}} - \text{EA}_{\text{ad}}$. We can also define a vertical threshold energy E_{vert} given by $\text{IP}_{\text{vert}} - \text{EA}_{\text{vert}}$. Above E_{vert} , we would expect the modified stripping mechanism to apply, since the electron jump is expected to be fast compared to the nuclear motions and would therefore give rise to a vertical, Frank-Condon transition to the ions. In the stripping model, the initial, vertical electron transfer puts $E_{\text{vert}} - E_{\text{ad}}$ internal energy into the products. Because the collision takes place at large impact parameters, little additional energy is transferred so that translational energy in excess of E_{vert}

(1) Hershbach, D. R. *Adv. Chem. Phys.* **1966**, *10*, 319. Hershbach, D. R. *J. Chem. Soc. Faraday Disc.* **1973**, *55*, 233.

(2) (a) Odiorne, T. J.; Brooks, P. R.; Kasper, J. V. V. *J. Chem. Phys.* **1971**, *55*, 1980. Pruett, J. G.; Grabiner, F. R.; Brooks, P. R. *J. Chem. Phys.* **1975**, *63*, 1173. (b) Heismann, F.; Loesch, H. J. *Chem. Phys.* **1982**, *64*, 43.

(3) Chupka, W. A.; Russell, M. E.; Refaey, K. *J. Chem. Phys.* **1968**, *48*, 1518. Chupka, W. A.; Russell, M. E. *J. Chem. Phys.* **1968**, *48*, 1527.

(4) Pruett, J. G.; Zare, R. N. *J. Chem. Phys.* **1976**, *64*, 1774.

(5) Alben, K. T.; Auerbach, A.; Ollison, W. M.; Weiner, J.; Cross, R. J. *J. Am. Chem. Soc.* **1978**, *100*, 3274.

(6) Hershberger, J. F.; McAndrew, J. J.; Cross, R. J.; Saunders, M. J. *J. Chem. Phys.* **1987**, *86*, 4916.

(7) Arena, M. V.; Hershberger, J. F.; McAndrew, J. J.; Cross, R. J.; Saunders, M. J. *J. Am. Chem. Soc.* **1987**, *109*, 6658-6663.

(8) Smith, D.; Adams, N. G. In *Gas Phase Ion Chemistry*; Bowers, M. T., Ed.; Academic Press: New York, 1979; Vol. 1, p 2. Gentry, W. R., In *Gas Phase Ion Chemistry*; Bowers, M. T., Ed.; Academic Press: New York, 1979; Vol. 2, p 221. Weglein, A. B.; Rapp, D. In *Gas Phase Ion Chemistry*; Bowers, M. T., Ed.; Academic Press: New York, 1979; Vol. 2, p 300. Lindinger, W. In *Gaseous Ion Chemistry and Mass Spectroscopy*; Futrell, J. H., Ed.; John Wiley and Sons: New York, 1986; p 141. Futrell, J. H. In *Gaseous Ion Chemistry and Mass Spectroscopy*; John Wiley and Sons: New York, 1986; pp 155, 201.

(9) Lacman, K.; Hershbach, D. R. *Chem. Phys. Lett.* **1972**, *6*, 106. Hubers, M. M.; Kleyn, A. W.; Los, J. *Chem. Phys.* **1976**, *17*, 303. Lacman, K. *Adv. Chem. Phys.* **1980**, *42*, 513.

(10) Lacman, K.; Maneira, M. J. P.; Moutinho, A. M. C.; Weigmann, U. *J. Chem. Phys.* **1983**, *78*, 1767.

(11) Russell, J. A.; Hershberger, J. F.; McAndrew, J. J.; Cross, R. J.; Saunders, M. J. *J. Chem. Phys.* **1985**, *82*, 2240.

[†] Present address: Department of Chemistry, Columbia University, New York, NY 10027.

[‡] Present address: Department of Chemistry, Brookhaven National Laboratory, Upton, NY 11937.

should go largely into translational energy of the products. We found this to be the case. In one case we also found that we could see reaction between E_{ad} and E_{vert} , but that the product contours had the forward-backward symmetry characteristic of a long-lived complex.

Here we use $\text{A} = \text{SnCl}_4$ and SbF_5 . SnCl_4 has vertical and adiabatic electron affinities of 1.18 ± 0.2 eV and 2.2 and 0.2 eV, respectively.¹⁰ The electron affinity of SbF_5 was unknown prior to our work, but, with use of the model describe above, we measured the vertical electron affinity of 1.3 ± 0.2 eV.¹¹ We use three amines for the electron donors: tetrakis(dimethylamino)ethylene (TDMAE) $[(\text{CH}_3)_2\text{N}]_2\text{C}=\text{C}[\text{N}(\text{CH}_3)_2]_2$ with vertical and adiabatic ionization potentials of 6.11 ± 0.02 eV and 5.36 ± 0.02 eV, respectively,¹² tri-*n*-butylamine (TBA) with vertical and adiabatic ionization potentials of 7.90 ± 0.02 eV and 6.98 ± 0.08 eV,¹³ and *tert*-butylbenzylamine (TBBA) with unknown ionization potentials. By chemically tuning the ionization potential and the electron affinity, we can check our model of the reaction over a range of values.

Experimental Section

The apparatus has been described previously^{6-8,14} so only a brief description will be given here. Each beam is formed in a Pyrex Nozzle 40–100 μm in diameter. The seed gas is introduced either by bubbling the carrier gas through the liquid seed to saturate it with the vapor or by injecting the liquid into the carrier gas with a motor-driven syringe. The beam has typically a few hundred mTorr of seed gas in an atmosphere of carrier gas. Three carrier gases were used: H_2 , He, and a mixture of 40% H_2 , 60% He. Each beam is formed in a chamber pumped by a 6-in oil diffusion pump. The two beams intersect at 90° or at 135° in the middle of the main vacuum chamber. Product ions are extracted by an ion lens system, mass selected by a quadrupole mass analyzer, and are detected by an electron multiplier.

Antimony pentafluoride is known to dimerize in the gas phase,¹⁵ and so our beam contains a small amount of dimer which can also react. By keeping the vapor pressure of SbF_5 low and the nozzle temperature above 270°C we can effectively eliminate the dimers. We cannot then vary the beam conditions to examine the effect of vibrational energy in the SbF_5 . In the case of SnCl_4 we find that H_2 in the carrier gas reduces the SnCl_4 and clogs the skimmer with a layer of metallic tin.

In a typical experiment,⁶ the product intensity is measured as a function of the temperature of the nozzle of the amine beam over a range of 30–400 $^\circ\text{C}$. This is done for each of the three carrier gases. We have mounted a filament directly over the beam intersection region. When turned on, electrons emitted from the filament ionize the beam, and we can measure the relative intensity of the beam under different conditions. We have found that the number density of the beam (mol/cm^3) is very nearly independent of the nozzle temperature provided the pressure behind the nozzle is held constant. There is a change in beam intensity as the carrier gas is changed, and this is included in the relative cross sections given here. We estimate a relative error of roughly 15% for the points with the same carrier gas, due largely to the drift in beam intensity during a run. There is an additional error of 15% for the normalization of cross sections of different carrier gases. The beam energy was calculated by using well-known formulas¹⁶ and included a correction for the nozzle slip factor. We estimate an error of roughly 0.4 eV. Since some of this is systematic error and is the same from run to run, we estimate that differences in relative energy are also accurate to 0.4 eV. The beam energy and its spread can be obtained experimentally by measuring the energy distribution of the ions formed by electron bombardment by using the filament. The measured and calculated distributions agree to within the above uncertainty. The spread in beam velocities is about 15% FWHM. If we assume that there is little vibrational relaxation in the nozzle expansion, then the vibrational energy can be calculated by using approximate formulas for heat capacity (see ref 6 for details). The vibrational energy depends on the nozzle temperature but is never more

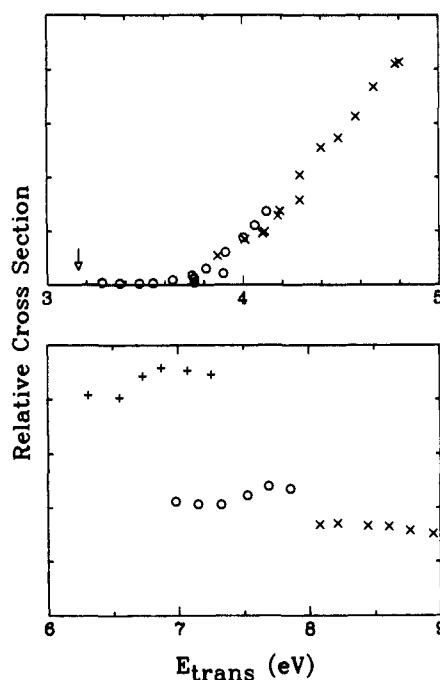


Figure 1. The cross section for electron transfer from TDMAE [tetrakis(dimethylamino)ethylene] to SnCl_4 plotted against relative translational energy. The top panel shows results by using a beam intersection angle of 90° and the bottom panel 135° . Three carrier gases are used: (+) He; (O) 40% H_2 and 60% He; and (x) H_2 . The nozzle temperature is varied over a range of 20–400 $^\circ\text{C}$ for each case. The arrow shows the adiabatic threshold energy of 3.16 eV.

than 0.5 eV. In fact, there is probably some relaxation of the low-frequency modes so that the vibrational energy is less than this.

Results

The relative cross section for electron transfer from TDMAE to SnCl_4 is shown in Figure 1. The top panel shows the cross section versus relative translational energy for the beams intersecting at 90° and the bottom panel for the beams intersecting at 135° . The cross sections for He carrier gas are indicated by (+), for the H_2/He mixture O, and for H_2 (x). In the 90° case the cross section for the He case is zero. In the 90° case we see that the cross section is independent of the type of carrier gas. This shows that vibrational energy plays only a minor role in the reaction since the vibrational temperature for the mixture is very much hotter than the vibrational temperature for H_2 at the same translational energy. The vertical arrow gives the adiabatic threshold energy of 3.16 ± 0.2 eV. The measured threshold of 3.7 ± 0.4 eV is within experimental error of this.

The bottom panel shows the results at 135° . Because of the larger beam intersection angle, the relative energy is higher than at 90° . The functional dependence of the cross section on translational and vibrational energy is also quite different from the low-energy case. The curves for the different carrier gases are now very different. The range of nozzle temperature in the three cases are the same so that corresponding points in the three cases have very nearly the same vibrational temperature. It is apparent, then, that the cross section drops rapidly as translational energy is raised. This decrease is well outside of the experimental error. As we go from low to high energy along any one of the three curves, the translational and vibrational energies both increase. The cross section is almost constant or rises slightly. If increasing translational energy causes the cross section to drop, then increasing vibrational energy must cause it to rise. This behavior is quite different from that observed in the halide abstraction reactions that we studied previously, where the cross section rises with translational energy and is almost independent of vibrational energy.

Figure 2 shows the corresponding data for $\text{SbF}_5 + \text{TDMAE}$. The data at 90° shows a lower threshold than for SnCl_4 . Furthermore the curves for the three carrier gases do not overlap.

(12) Nakato, Y.; Ozaki, M.; Egawa, A.; Tsubomura, H. *Chem. Phys. Lett.* **1971**, *9*, 615.

(13) Aue, D. H.; Webb, H. M.; Bowers, M. T. *J. Am. Chem. Soc.* **1976**, *98*, 311. Aue, D. H.; Bowers, M. T. *Gas Phase Ion Chemistry*, Bowers, M. T., Ed.; Academic Press: New York, 1979.

(14) Lee, L.; Russell, J. A.; Su, R. T. M.; Cross, R. J.; Saunders, M. J. *Am. Chem. Soc.* **1981**, *103*, 5031. Russell, J. A.; Hershberger, J. F.; McAndrew, J. J.; Cross, R. J.; Saunders, M. *J. Phys. Chem.* **1984**, *88*, 4494.

(15) Lawless, E. W. *Inorg. Chem.* **1971**, *10*, 2084. Vasile, M. J.; Jones, G. R.; Falconer, W. E. *Adv. Mass Spectrom.* **1974**, *6*, 557.

(16) Anderson, J. B. *Molecular Beams and Low Density Gas Dynamics*; Wegener, P. P., Ed.; 1974.

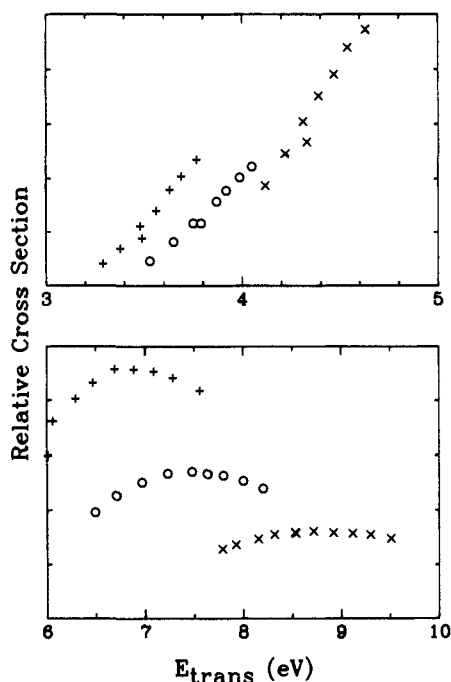


Figure 2. The cross section for electron transfer from TDMAE to SbF_5 .

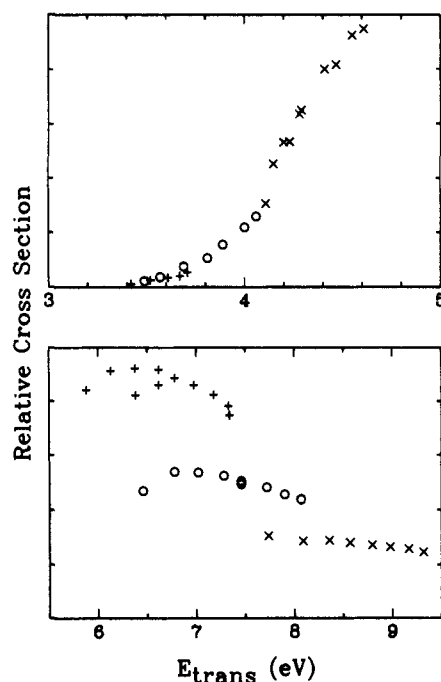


Figure 4. The cross section for electron transfer from TBA to SbF_5 .

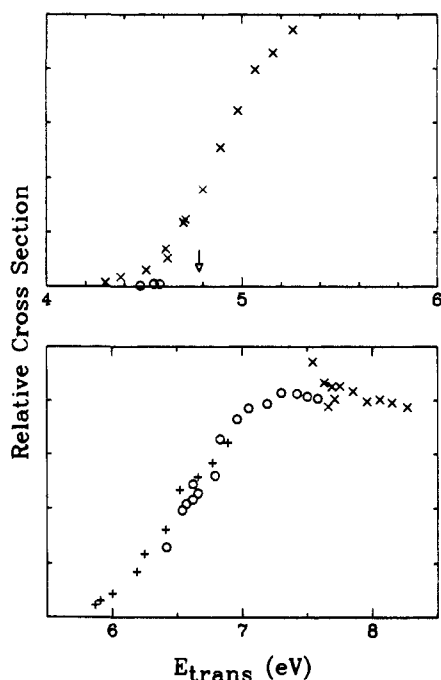


Figure 3. The cross section for electron transfer from TBA (tri-*n*-butylamine) to SnCl_4 . The adiabatic threshold is 4.78 eV.

The cross section for He carrier gas, which has the highest vibrational temperature at a given translational energy, is the highest. This shows that vibrational energy in TDMAE enhances the charge exchange. The case seems to be intermediate between the 90° and 135° cases for SnCl_4 . The three curves nearly overlap if we plot the cross section versus the total (translational plus vibrational) energy. This shows that the two are of comparable importance in this energy region. At 135° there is extensive fragmentation of the TDMAE^+ product. The data shown in the bottom panel show the cross section for the production of all the positive ions (parent plus fragments). The same trends are evident that we saw in the case of SnCl_4 : increasing translational energy decreases the cross section, and increasing vibrational energy increases it. SbF_5 evidently has a higher electron affinity than SnCl_4 , and this has the effect of shifting all the curves to lower energies.

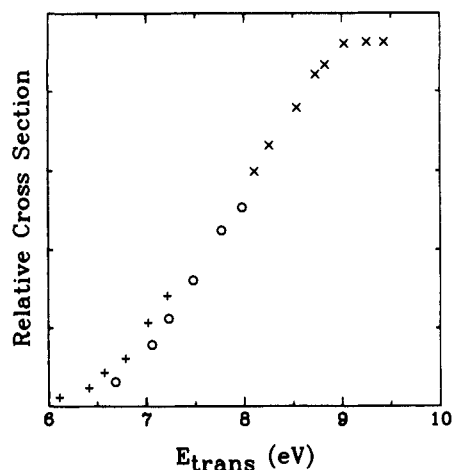


Figure 5. The cross section for electron transfer from TBBA (*tert*-butylbenzyl amine) to SnCl_4 . Only the data for 135° beam intersection angle is shown because the data at 90° is all below the threshold.

Figure 3 shows the data for $\text{SnCl}_4 + \text{TBA}$. Because the ionization potential of TBA is higher than that for TDMAE, the data are all shifted to higher energy. The threshold is 4.5 ± 0.4 eV, 0.8 eV higher than for TDMAE, so that only the points for H_2 carrier gas lie above it. The data for 135° show a single curve for the three carrier gases which rises and then peaks. This would appear to be intermediate between the two parts of Figure 1. It is not clear why the threshold is higher for the 135° case. Figure 4 shows the data for $\text{SbF}_5 + \text{TBA}$. The data closely resemble those for $\text{SnCl}_4 + \text{TDMAE}$. Evidently, the decrease in electron affinity is approximately made up for by the increase in ionization potential of the amine. If we can equate the threshold of the reaction, 3.6 ± 0.4 eV, with the adiabatic threshold for the reaction, then we obtain a value of 3.4 ± 0.4 eV for the adiabatic electron affinity of SbF_5 , 1.2 eV higher than that for SnCl_4 .

Figure 5 shows the data for $\text{SnCl}_4 + \text{TBBA}$. Only the data for 135° are shown since the whole energy region covered by the 90° case is below the threshold. The data look very much like the 90° data for $\text{SnCl}_4 + \text{TDMAE}$ shifted up in energy. Again, if we can equate the threshold of 6.5 ± 0.4 eV with the adiabatic threshold energy, we obtain an adiabatic ionization potential of 8.7 ± 0.4 eV for TBBA. Figure 6 shows the data for $\text{SbF}_5 + \text{TBBA}$. Again most of the 90° energy range is below the threshold,

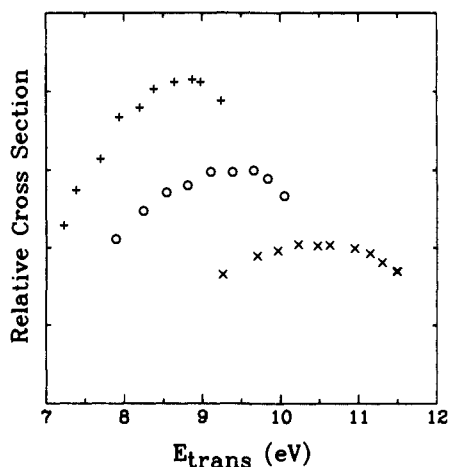


Figure 6. The cross section for electron transfer from TBBA to SbF_5 . Only the data for 135° beam intersection angle is shown.

and so it is not shown. As might be expected from the structure of the amine, we observe extensive production of fragment ions as well as the parent ion. The data in Figure 5 show the cross section for the total ion formation.

In the cases of TDMAE and TBBA the cation product can dissociate, and several fragment ions are observed. In the case of TDMAE, these involve loss of methyl groups and loss of dimethylamino radicals. The case of TBBA is more interesting, and that is why it was chosen. Figure 7 shows the fraction of each product ion produced as a function of the translational energy for the reaction of $\text{SbF}_5 + \text{TBBA}$ at 135° . It should be pointed out that we are using a quadrupole mass filter, and therefore the transmission efficiency depends slightly on the mass of the ion. The relative ion intensities may be in error by 10–20% because of this. In addition to the parent ion (P), we see four fragments: loss of a methyl group $[\text{PhCH}_2\text{NHC}(\text{CH}_3)_2]^+$ (A), loss of butyl radical $[\text{PhCH}_2\text{NH}]^+$ (B), C_7H_7^+ (C), and C_4H_9^+ (D). The loss of a methyl group gives a cation where the charge can be distributed to the nitrogen and the adjacent butyl carbon. Similarly, the loss of butyl radical and the possible migration of one of the α hydrogens to the nitrogen produces an ion where the positive charge can be distributed between the nitrogen, the α carbon, and the ortho and para ring carbons. C_7H_7^+ may be the very stable tropylium or benzyl cations (we cannot determine the structure). C_4H_9^+ is almost certainly the very stable *tert*-butyl carbocation.

Several features of the fragmentation are immediately obvious. The extent of fragmentation is large; above 11 eV, the parent ion accounts for less than 10% of the product. All the curves are independent of the type of carrier gas so that vibrational energy plays a minor role in the fragmentation process. This result is very surprising. As Figure 6 clearly shows, the cross section for the electron transfer depends very strongly on vibrational energy in TBBA, yet once the electron has jumped, the fate of the cation is independent of the vibrational energy. This behavior is very different from the fragmentation observed in the halide abstraction reaction where the cross section for the halide abstraction is nearly independent of vibrational energy, but the fragmentation depends strongly on it.

Discussion

The data for all six cases follow a similar pattern. At low energies there is a sharp rise in the cross section above the threshold. The cross section peaks and shows increasing dependence on vibrational energy in the amine. Finally, at high energy the cross section decreases with increasing translational energy but increases with increasing vibrational energy. The different systems exhibit these regions at different energies depending on the ionization potential of the electron donor amine and the electron affinity of the acceptor.

The behavior is not unexpected from all that is known about charge transfer. We must have at least two potential-energy surfaces, one covalent corresponding to the reactants and one ionic

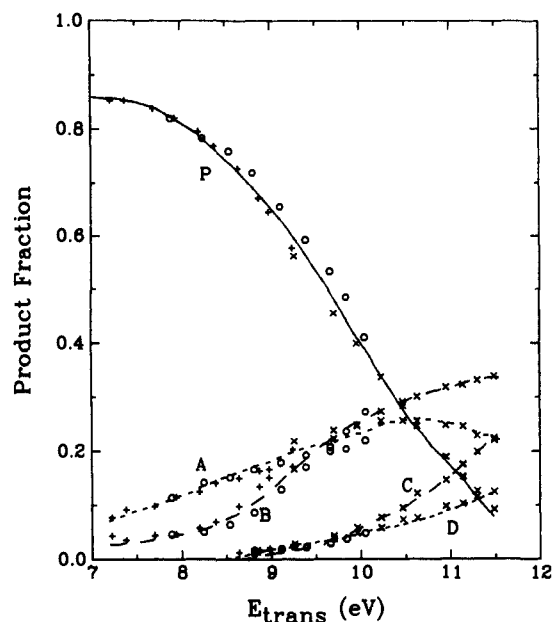


Figure 7. The fraction of all cations observed in the various products for the reaction of SbF_5 and TBBA: P, parent TBBA^+ ; A, loss of a methyl group $[\text{PhCH}_2\text{NHC}(\text{CH}_3)_2]^+$; B, loss of butyl radical $[\text{PhCH}_2\text{N}]^+$ (or an isomer); C, C_7H_7^+ ; D, C_4H_9^+ . The lines are smoothed curves drawn through the data to distinguish the different data sets.

corresponding to the products. The covalent surface is probably relatively flat until the two molecules are close to each other, and then it becomes sharply repulsive. The ionic surface is higher asymptotically than the covalent surface—the reaction is endothermic by a few eV. The surface, however, is strongly attractive due to the Coulomb force. Because the adiabatic and vertical ionization potentials and electron affinities differ from each other, we know that the structures of the ions and neutrals are different, and therefore the difference in energy between the two surface depends on one or more vibrational coordinates. This means that the “seam” where the two surfaces cross must depend on vibrational coordinates as well as on the intermolecular distance R .

Below the adiabatic threshold (E_{ad}) an electron can still jump between D and A. The pair of ions formed, however, does not have enough energy to escape from the Coulomb well. Eventually, the ion pair complex will cross back to the covalent surface and dissociate as neutrals. We cannot see this channel. The region between the adiabatic and vertical thresholds presents several problems. If the electron jump is fast, it should be a near vertical process. This would leave the ion pair with insufficient energy to dissociate unless internal energy in the ions were to be transferred into the Coulomb mode (which goes into translational energy of the products). Now, the Coulomb mode has a very low force constant and a long period. Because of this frequency mismatch, it is difficult to transfer energy from the fast vibrations of the ions into the Coulomb mode. In $\text{SnCl}_4 + \text{TDMAE}$ there are 117 vibrational degrees of freedom and only one Coulomb mode. Simple considerations of the RRKM theory would dictate that the energy would tend to flow out of the Coulomb mode not into it. Perhaps the small number of products results from a jump to the ground and low-lying vibrational states of the ions with low but finite Franck–Condon factors. One would expect in this case that the cross section would depend strongly on vibrational energy in the modes which connect the neutrals to the ions. We observe no strong vibrational dependence on the cross section, but perhaps, with so many modes, the effect is diluted out.

Above the vertical threshold E_{vert} the reaction can take place in a direct process—our studies on the product distributions show this. The crossing seam lies at $R \approx 3 \text{ \AA}$. The electron must then move a large distance while the nuclei are in the immediate vicinity of the crossing seam. At the high energies of our experiment, it cannot always make the jump. The simple Landau–Zener formula predicts that at high energy the probability is proportional to v^{-2} ,

where v is the local velocity going through the crossing seam. In our case the simple Landau-Zener theory is not adequate since the position of the crossing seam depends on vibration, but we do see a rapid drop in the cross section with increasing translational energy as is predicted by the theory. Because the crossing seam depends on vibration, the cross section can be expected to depend on the initial vibrational energy, although it is difficult to predict which way the dependence will go.

The fragmentation results present other interesting problems. According to the modified stripping model which works well for the energy distributions of the products, any translational energy in excess of the vertical threshold goes into translational energy of the product ions. This implies that the product ions are formed with a constant internal energy ($E_{\text{vert}} - E_{\text{ad}}$) independent of the initial translational energy. The fragment ratios should then be independent of translational energy. The results in ref 11 which confirm this model were done on $\text{SbF}_5 + \text{TDMAE}$ at energies below 6.1 eV, below the lowest energies in Figure 7. It is possible that the much higher ionization potential of TBBA requires a much harder collision for the reaction to occur. In the case of TBBA the energy required for dissociation of the ion product is quite small so only a small fraction of the initial translational energy is required. The fact that reactant vibrational energy does not affect the dissociation may indicate that the dissociation occurs immediately after the electron transfer in a direct process. Since

the amount of vibrational energy in the reactants is much smaller than the amount of translational energy, we may simply not be able to see the effect. It may be that the choice of products depends on more than one ionic surface. Thus the system can miss the first jump, remain on the covalent surface, and then jump to an ionic surface which is dissociative asymptotically. It is very difficult to estimate the absolute cross section for out reactions, but we guess that it is in the range of 10^{-3} – 10^{-1} Å² depending on the system and energy. This is small enough so that many nonionic processes can occur at the same time as the electron-transfer reaction.

Our experimental results fall into a simple pattern which is in qualitative agreement with what is known about charge transfer and chemical dynamics. The results are quite different from those obtained for the halide transfer reaction 1. The cross sections for the halide transfer may be very sensitive to vibration near the threshold but are insensitive at higher energies. When fragmentation occurs, the product ratios depend very strongly on vibrational energy in the reactants.

Acknowledgment. Research support from the National Science Foundation under Grant CHE-8201164 is gratefully acknowledged.

Registry No. TBA, 102-82-9; TBBA, 3378-72-1; TDMAE, 996-70-3; SbF_5 , 7783-70-2; SnCl_4 , 7646-78-8.

Homotropylium Cation Revisited: POAV and 3D-HMO Analysis

R. C. Haddon

Contribution from AT&T Bell Laboratories, Murray Hill, New Jersey 07974.
Received March 16, 1987

Abstract: Homoconjugate bonding was characterized as: "... orbital overlap of a type intermediate between σ and π ", by Winstein over 30 years ago. Nevertheless, the concept has remained controversial and the molecular and electronic structure of the homotropylium cation (**1**, the prima facie example of this phenomenon) remains in doubt. Previous theoretical calculations and experimental studies of derivatives of the molecule have produced evidence for two minima on the potential surface, with homoconjugate bond distances $R_{1,7} = 1.6$ and 2.3 Å. In the present paper we report the results of Hartree-Fock (HF) geometry optimizations of the molecular structure of **1**. At the HF level the same two minima are located, but when electron correlation effects are included in the wave function, the potential surface is totally transformed and a single minimum results with an $R_{1,7}$ value of 1.7 – 2.0 Å. The structures obtained by calculation are further analyzed with the POAV and 3D-HMO theories. This allows the development of a unified picture of homoaromatic character as embodied in **1**. The results of the analysis provide a natural explanation of the molecular and electronic structure of the homotropylium cation, the distance dependence of the homoconjugate bond, the electronic spectrum, and the ring current as observed in the NMR chemical shifts and diamagnetic susceptibility exaltation. The concept of homoaromatic character as embodied in the homotropylium cation is supported by this study. The present analysis differs with all previous experimental interpretations and calculations as to the details.

Homoaromatic character has proved to be a particularly enduring concept in organic chemistry.¹ Qualitative molecular orbital theories²⁻⁴ provided a satisfactory account of the occurrence

(and nonoccurrence) of this phenomenon some time ago, but quantitative data have proved elusive.

The best characterized homoaromatic species at the present time is probably the homocyclopropenylium cation.⁵ An X-ray crystal structure⁶ of a simple derivative yielded a homoaromatic bond length of 1.775 Å, and an NMR study⁷ of the parent system provided a bridge-flipping barrier of 8.4 kcal/mol. These parameters were fairly well reproduced by semiempirical MINDO

(1) Review: (a) Winstein, S. *Spec. Publ.-Chem. Soc.* **1967**, No. 21, 5; *Q. Rev. Chem. Soc.* **1969**, 23, 141. (b) Brown, R. S.; Traylor, T. G. *J. Am. Chem. Soc.* **1973**, 95, 8025. (c) Warner, P. M. In *Topics in Nonbenzenoid Aromatic Character*; Nozoe, T., Breslow, R., Hafner, K., Ito, S., Murata, I., Eds.; Hirokawa: Tokyo, 1976; Vol. 2. (d) Paquette, L. A. *Angew. Chem., Int. Ed. Engl.* **1978**, 17, 106. (e) Childs, R. F. *Acc. Chem. Res.* **1984**, 17, 347.

(2) (a) Haddon, R. C. *Tetrahedron Lett.* **1974**, 2797. (b) Haddon, R. C. *Ibid.* **1974**, 4303. (c) Haddon, R. C. *Ibid.* **1975**, 863. (d) Haddon, R. C. *J. Am. Chem. Soc.* **1975**, 97, 3608. (e) Haddon, R. C. *Aust. J. Chem.* **1977**, 30, 1. (f) Haddon, R. C.; Roth, H. D. *Croat. Chem. Acta* **1984**, 57, 1165.

(3) Hehre, W. J. *J. Am. Chem. Soc.* **1974**, 96, 5207.

(4) (a) Jorgensen, W. L.; Borden, W. T. *J. Am. Chem. Soc.* **1973**, 95, 6649. (b) Jorgensen, W. L. *Ibid.* **1975**, 97, 3082. (c) Jorgensen, W. L. *Ibid.* **1976**, 98, 6784.

(5) (a) Applequist, D. E.; Roberts, J. D. *J. Am. Chem. Soc.* **1956**, 78, 4012. (b) Woods, W. G.; Carboni, R. A.; Roberts, J. D. *Ibid.* **1956**, 78, 5653. (c) Kiefer, E. F.; Roberts, J. D. *J. Am. Chem. Soc.* **1962**, 84, 784.

(6) Krüger, C.; Roberts, P. J.; Tsay, Y.-H.; Koster, J. B. *J. Organomet. Chem.* **1974**, 78, 69.

(7) (a) Olah, G. A.; Staral, J. S.; Liang, G. *J. Am. Chem. Soc.* **1974**, 96, 6233. (b) Olah, G. A.; Staral, J. S.; Spear, R. J.; Liang, G. *Ibid.* **1975**, 97, 5489.